NASA Contractor Report 178089

ICASE REPORT NO. 86-21

ICASE

A FOURTH ORDER ACCURATE FINITE DIFFERENCE SCHEME FOR THE COMPUTATION OF ELASTIC WAVES

A. Bayliss

K. E. Jordan

B. J. LeMesurier

E. Turkel

Contract Nos. NAS1-17070, NAS1-18107

April 1986

INSTITUTE FOR COMPUTER APPLICATIONS IN SCIENCE AND ENGINEERING
NASA Langley Research Center, Hampton, Virginia 23665

Operated by the Universities Space Research Association

National Aeronautics and
Space Administration

Langley Research Center
Hampton, Virginia 23665

A FOURTH ORDER ACCURATE FINITE DIFFERENCE SCHEME FOR THE COMPUTATION OF ELASTIC WAVES

A. Bayliss
Exxon Corporate Research Science Laboratories

K. E. Jordan
Exxon Research and Engineering Company

B. J. LeMesurier
New York University

E. Turkel
Tel Aviv University and
Institute for Computer Applications in Science and Engineering

ABSTRACT

A finite difference model for elastic waves is introduced. The model is based on the first order system of equations for the velocities and stresses. The differencing is fourth order accurate on the spatial derivatives and second order accurate in time. The model is tested on a series of examples including the Lamb problem, scattering from a plane interfaces and scattering from a fluid-elastic interface. The scheme is shown to be effective for these problems. The accuracy and stability is insensitive to the Poisson ratio. For the class of problems considered here we find that the fourth order scheme requires from two-thirds to one-half the resolution of a typical second order scheme to give comparable accuracy.

This work was partially supported under the National Aeronautics and Space Administration under NASA Contract Nos. NAS1-17070 and NAS1-18107 while the fourth author was in residence at the Institute for Computer Applications in Science and Engineering (ICASE), NASA Langley Research Center, Hampton, VA 23665.

Introduction

In this paper we introduce and validate a fourth order accurate finite difference scheme for the computation of waves in an elastic medium. The method is based on the first order system for the linearized velocities and stresses. The numerical scheme is a fourth order accurate version of the MacCormack scheme (see Gottlieb and Turkel, 1976) which has been shown to be effective for acoustic wave propagation (Maestrello et. al., 1981).

In this paper we consider only the heterogeneous formulation, where variable, possibly discontinuous, elastic parameters are used and the equation is differenced over the entire computational domain. For a discussion of the differences between the heterogeneous formulation and the homogeneous formulation in which interface conditions are explicitly imposed we refer to (Kelly et. al., 1976). In (Kelly et. al., 1976) a second order accurate scheme for the coupled system of wave equations obtained from the displacement formulation of elastodynamics is introduced. We refer to this as the (2-2) scheme since it is second order accurate in time and second order accurate in space. This scheme is commonly used in seismological applications and we will directly compare the proposed fourth order scheme with the (2-2) scheme. The proposed scheme is second order accurate in time and fourth order accurate in space. It will be referred to as a (2-4) scheme.

The first order system has been used previously to compute elastic waves. The reader is referred to (Clifton, 1967), (Madariaga, 1976), (Virieux and Madriaga, 1982) and (Emerman et. al., 1982) for a discussion of some schemes that have been used previously. All of the above schemes are only second order accurate in space and are there-

fore distinctly different from the scheme proposed here. It is possible to extend the (2-2) scheme of (Kelly et. al., 1976) to make the spatial differences fourth order accurate. This is similiar to the derivation of fourth order accurate schemes for the wave equation (see for example (Alford et. al., 1974)). Such a fourth order accurate scheme has been used for acoustic and S-H wave propagation (see for example (Frankel and Clayton, 1984)). The extension to the system of coupled wave equations for an elastic medium is somewhat more complicated, due to the presence of the mixed derivatives but in practice would be relatively straightforward.

As far as we are aware, no such (2-4) scheme has been studied for elastic wave propagation. A major source of difficulty is in obtaining a stable implementation of the free surface condition which is of sufficient accuracy to maintain the overall fourth order accuracy of the scheme (see (Oliger, 1976) for a discussion of the importance of the numerical approximation of boundary conditions). The need to approximate one-sided derivatives for the free surface conditon is a major numerical difference between elastodynamics and acoustics where the pressure release boundary conditon does not involve spatial derivatives. The scheme proposed here, for which the stresses are dependent variables, permits a stable and accurate implementation of the free surface condition even for large Poisson ratios (see below).

A higher order accurate scheme (in fact infinite order accurate) has been proposed by (Kosloff et. al., 1984). This method is based on the Fourier pseudo-spectral method and requires a periodic extension of the computational domain. The comparison between this method and the (2-4) scheme proposed here remains to be carried out,

in particular for realistic size seismological models involving discontinuous elastic parameters.

The proposed (2-4) scheme is based on operator splitting where the two-dimensional equations are solved first in one dimension and then in the second. The concept of operator splitting and the details of the (2-4) scheme are discussed in the next section. We then present numerical examples for the Lamb problem, scattering from a horizontal interface and scattering from a fluid-elastic interface. We finally present our conclusions.

NUMERICAL SCHEME

This section is divided into four parts. In part A we discuss the formulation of linear elastodynamics as a first order system for the velocities and stresses. In part B, the numerical scheme is described. In part C, we consider the choice of timestep and in part D the boundary conditions are described.

A. Formulation

The equations of linear isotropic elastodynamics in Cartesian coordinates are

$$\begin{aligned} \rho u_t &= \tau_{11,x} + \tau_{12,y} \\ \rho v_t &= \tau_{12,x} + \tau_{22,y} \\ \tau_{11,t} &= (\lambda + 2\mu)u_x + \mu v_y \\ \tau_{22,t} &= \mu u_x + (\lambda + 2\mu)v_y \\ \tau_{12,t} &= \mu(v_x + u_y). \end{aligned} \tag{1}$$

In equation (1) u and v are the horizontal and vertical velocities respectively, τ_{ij} are the components of stress tensor. The elastic parameters are the density ρ and the Lame constants λ and μ. The compressional and shear wave speeds C_p and C_s are given by

$$\begin{aligned} C_p^2 &= \frac{(\lambda + 2\mu)}{\rho} \\ C_s^2 &= \frac{\mu}{\rho} \end{aligned} \tag{2}$$

and $C_p > C_s$.

Associated with these speeds there are the spatial wavelengths $\lambda_p = C_p/f$, $\lambda_s = C_s/f$ where f is a characteristic frequency. Hence

$$\frac{\lambda_p}{\lambda_s} = \frac{C_p}{C_s} > 1. \tag{3}$$

The Poisson ratio is given by

$$\nu = \frac{1}{2}\left[\frac{1 - 2C_s^2/C_p^2}{1 - C_s^2/C_p^2}\right] \tag{4}$$

so that

$$\frac{C_p^2}{C_s^2} = \frac{2(1-\nu)}{1-2\nu} . \tag{5}$$

For seismic problems it is frequently assumed that ν is around 0.25 and thus that $C_p/C_s=\sqrt{3}$. It then follows that the shear wavelengths are about 60% smaller than the compressional wavelengths. Therefore the spatial resolution requirements must be based on the shorter shear wavelengths. In addition there exist interface and surface waves which generally have smaller wavelengths than the shear waves. There are applications where these waves are not generally considered to be important. Nevertheless, it is necessary to resolve these waves sufficiently well to prevent a spurious transfer of energy into other wave modes. We also do not want numerical dispersion for these waves to interfere with the generation and interpretation of the waves of interest. In some cases, e.g. weathering layers, the Poisson ratio can be considerably larger that 0.25. This further accentuates the difference in resolution requirements between shear and compressional waves.

For convenience we write equation (1) in vector form

$$W_t = AW_x + BW_y \tag{6}$$

where $W = (u, v, \tau_{11}, \tau_{22}, \tau_{12})^T$ and the matrices A and B are given by

$$A = \begin{pmatrix} 0 & 0 & \frac{1}{\rho} & 0 & 0 \\ 0 & 0 & 0 & 0 & \frac{1}{\rho} \\ \rho C_p^2 & 0 & 0 & 0 & 0 \\ \rho C_s^2 & 0 & 0 & 0 & 0 \\ 0 & \rho C_s^2 & 0 & 0 & 0 \end{pmatrix}$$

$$B = \begin{pmatrix} 0 & 0 & 0 & 0 & \frac{1}{\rho} \\ 0 & 0 & 0 & \frac{1}{\rho} & 0 \\ 0 & \rho C_s^2 & 0 & 0 & 0 \\ 0 & \rho C_p^2 & 0 & 0 & 0 \\ \rho C_s^2 & 0 & 0 & 0 & 0 \end{pmatrix}$$

We can also write equation (6) as a symmetric system

$$E_0 W_t = A_0 W_x + B_0 W_y \qquad (7)$$

where

$$E_0 = \begin{pmatrix} \rho & 0 & 0 & 0 & 0 \\ 0 & \rho & 0 & 0 & 0 \\ 0 & 0 & \frac{\lambda+2\mu}{(\lambda+2\mu)^2-\mu^2} & \frac{-\mu}{(\lambda+2\mu)^2-\mu^2} & 0 \\ 0 & 0 & \frac{-\mu}{(\lambda+2\mu)^2-\mu^2} & \frac{\lambda+2\mu}{(\lambda+2\mu)^2-\mu^2} & 0 \\ 0 & 0 & 0 & 0 & \frac{1}{\mu} \end{pmatrix}$$

$$A_0 = \begin{pmatrix} 0 & 0 & 1 & 0 & 0 \\ 0 & 0 & 0 & 0 & 1 \\ 1 & 0 & 0 & 0 & 0 \\ 0 & 0 & 0 & 0 & 0 \\ 0 & 1 & 0 & 0 & 0 \end{pmatrix}$$

$$B_0 = \begin{pmatrix} 0 & 0 & 0 & 0 & 1 \\ 0 & 0 & 0 & 1 & 0 \\ 0 & 0 & 0 & 0 & 0 \\ 0 & 1 & 0 & 0 & 0 \\ 1 & 0 & 0 & 0 & 0 \end{pmatrix}$$

We note that the matrices $E_0^{-1}A_0$ and $E_0^{-1}B_0$ do not commute. Since ρ, λ, μ are independent of time, E_0 is also independent of time. The matrices A_0 and B_0 are also independent of the spatial coordinates. It follows that equation (7) can be be written in the general form

$$U_t = f_x + h_y \tag{8}$$

where the vector U is E_0W and the functions f and h are A_0W and B_0W respectively. Equations of the form of (8) are called divergence-free. We will develop a numerical scheme for equations of this form. Since equation (7) was obtained from equation (6) by linear manipulations the resulting scheme will be valid for equation (6). The numerical code is based on equation (6).

B. Numerical Algorithm

The numerical algorithm will be based on the method of dimensional splitting (Strang, 1968). In this method, the two-dimensional equation (6) is updated for one timestep by first solving the equation in the x-direction and then in the y direction. For the next timestep the order of the x and y updates is reversed. In order to advance the solution from time level n to level n+2 we use the formula

$$W^{n+2} = L_xL_yL_yL_xW^n; \tag{9}$$

L_x,L_y represent the solution to the one dimensional problems

$$W_t = AW_x$$
$$W_t = BW_y \qquad (10)$$

respectively.

It follows from equation (8) that to advance the solution one timestep we solve equation (6) using only the terms involving the x-derivatives. We then use these new values for the dependent variables and solve equation (6) using only the terms involving the y-derivatives. This gives the solution at time level n+1. To update to the next time level we repeat the procedure but reverse the order of the x and y updates. By reversing the order the resulting scheme is second order accurate in time.

The use of operator splitting has the following advantages.

(a) The maximum allowed timestep is governed by the associated one-dimensional equations. The allowed timestep is larger than for unsplit schemes.

(b) split schemes are particularly well suited to multi-processing (see Schenck et. al.,1985)). For example in the first step all the x updates for each line y = constant can be done independently.

(c) split schemes tend to have smaller phase errors than schemes (Turkel, 1974).

The proposed scheme can be implemented without splitting if desired (see (Gottlieb and Turkel, 1976)).

We need to specify a one-dimensional scheme for the operators

L_x and L_y. We use a scheme that is second order in time and fourth order in space (Gottlieb and Turkel, 1976). For the equation

$$U_t = f_x \tag{11}$$

we use

$$\bar{U}_i = U_i^n + \frac{\Delta t}{6\Delta x}\left(7(f_{i+1}^n - f_i^n) - (f_{i+2}^n - f_{i+1}^n)\right)$$

$$U_{i+1}^{n+1} = \frac{1}{2}\left(U_i^n + \bar{U}_i + \frac{\Delta t}{6\Delta x}\left(7(\bar{f}_i - \bar{f}_{i-1}) - (\bar{f}_{i-1} - \bar{f}_{i-2})\right)\right) \tag{12}$$

alternating with a symmetric variant. In equation (12) the subscript 'i' denotes the spatial grid point and the superscript 'n' denotes the time level. The resulting scheme is stable when applied to equation (6) provided

$$\frac{\Delta t}{\Delta x} C_p \leq .67 \ . \tag{13}$$

The ratio on the left hand side of equation (13) will be called the CFL number.

The scheme described by equation (12) together with operator splitting has been applied successfully to a variety of wave propagation problems. The reader is referred to (Maestrello et. al., 1981) for an application to the computation of acoustic disturbances in a jet. As far as we are aware, split schemes have not yet been applied to elasto-dynamic problems. The scheme based on equation (12) is dissipative and damps the high frequencies (Gottlieb and Turkel, 1976). It has a greatly reduced truncation error compared to second order schemes.

The order of accuracy in time is second order. Hence, one achieves true fourth order accuracy only if $\Delta t = 0(\Delta x^2)$. Thus in gen-

eral the timestep must be smaller than the maximum timestep allowed by stability (equation (13)) in order to prevent the errors due to the second order accuracy in time from dominating the truncation error. In elastic wave propagation, however, it is possible to choose a timestep near that allowed by stability. This is due to the difference in size between the compressional and shear velocities. We have verified this by extensive numerical experiments and provide a justification of this immediately below.

C. Choice of Timestep

In elasticity the spatial resolution and the timestep are chosen according to two different considerations. This is because of the existence of two different characteristic speeds. In general, the spatial resolution is based on the shear velocity while the stability restriction , equation (13), is based on the larger compressional velocity. This allows larger timesteps without losing temporal accuracy.

In order to see this let f be a characteristic frequency of the problem so that the associated compressional and shear wavelengths satisfy equation (3). Assume that we could completely decouple the compressional and shear waves and use a different mesh size for each wave type that is appropriate to obtain a specified accuracy. The timesteps for each wave type would then be determined by

$$\frac{\Delta t}{\Delta x_p} = \frac{K}{C_p}$$
$$\frac{\Delta t}{\Delta x_s} = \frac{K}{C_s} \qquad (14)$$

where K is the CFL number. For the scheme described in equation (12) the maximum value of K allowed by stability is 0.67. In order to

reduce temporal errors by reducing the timestep, K is reduced. It follows from equation (14) that

$$\frac{\Delta x_p}{\Delta x_s} = \frac{C_p}{C_s} \tag{15}$$

This is simply a statement that a smaller mesh is required to resolve shear waves. In practice we must use the same mesh, Δx_s, for both compressional and shear waves. Since the timestep for the system is based only on C_p according to equation (13) we have

$$\Delta t = \frac{K' \Delta x_s}{C_p} \tag{16}$$

where K' is the CFL number used in the actual computation. Comparing equation (14) with equation (16) we find that

$$K' = \frac{K C_p}{C_s} . \tag{17}$$

According to equation (17) the CFL number that is actually used in the code (K') is equal to the CFL number based on temporal accuracy (K) multiplied by $C_p/C_s(\sim\sqrt{3})$. Hence we should choose the timestep to be about 60% larger than the timestep that would give acceptable results for the compressional and shear waves decoupled. It is clear from this argument that the compressional waves will generally be oversampled but this is unavoidable for any scheme that solves the equation (1).

It follows from the discussion above that the spatial mesh size is governed by the shear velocity while the explicit timestep restriction due to stability is governed by the larger compressional velocity. This is essentially the case for all explicit finite difference schemes. For a scheme that is second order accurate in both

space and time, the optimal timestep is usually the maximum allowed by stability. For a scheme that is second order accurate in time and fourth order accurate in space the optimum time step is typically smaller than that allowed by stability. This is in order to prevent the second order temporal errors from dominating the truncation error. However when the explicit timestep restriction itself forces a small timestep, the (2-4) scheme can be run at or near its stability limit and the temporal errors will be negligible. The use of operator splitting then permits a larger timestep as indicated above.

As the Poisson ratio increases the ratio of the compressional velocity to the shear velocity becomes larger. The corresponding timestep forced by the stability restriction can become much smaller than that required for accuracy. We have found that for a Poisson ratio around 0.3 the (2-4) scheme can be run at its stability limit (equation (13)) with little degradation in accuracy. For very high Poisson ratios, implicit schemes such as that proposed by (Emerman et. al., 1982) would become more efficient since they would permit timesteps that are not restricted by stability. In practice this must be balanced against the additional work per timestep required by implicit schemes. This discussion highlights a difference between elasticity and acoustics or S-H wave propagation that makes (2-4) schemes more efficient in the elastic case. The discussion would be applicable to acoustic wave propagation only if the computational model included wide variations in the size of the acoustic velocity.

The numerical experiments using this (2-4) scheme were performed in a rectangular region

$$0 \le x \le L_1 ; \; -L_2 \le y \le 0. \qquad (18)$$

A Cartesian mesh with $\Delta x = \Delta y$ is always used independent of the shape of

the interfaces. It requires 112 floating point operations per grid point (multiplications and adds) to advance the solution from t to $t+\Delta t$ (ignoring boundary calculations). The simplicity of the algorithm and the mesh makes it easy to treat many different applications. Changes in geometry or even in the equations do not introduce any significant complications.

D. Boundary Conditions

The interior scheme, given by equation (12) requires the use of two points in every direction from the point being advanced. At boundaries some numerical boundary treatment must be introduced because the boundary point does not have enough neighbors to implement the scheme. In addition, there are physical boundary conditions that must be imposed.

In each sweep all boundary fluxes are defined at points outside of the computational domain by a third order extrapolation. For example, for the scheme defined by equation (12) if i=n is a boundary point we define,

$$\begin{aligned} f_{n+1} &= 4f_n - 6f_{n-1} + 4f_{n-2} - f_{n-3} \\ f_{n+2} &= 4f_{n+1} - 6f_n + 4f_{n-1} - f_{n-2} \end{aligned} \tag{19}$$

The extrapolated fluxes f_{n+1} and f_{n+2} are used to complete the forward predictor. Other boundaries are treated similarly. The third order extrapolation given by equation (17) enables us to compute a solution at the boundary which maintains the overall fourth order accuracy of the scheme. It is shown in (Oliger, 1976) that the accuracy obtained from fourth order accurate interior schemes can be significantly degraded if a third order accurate boundary treatment is not used.

It remains to impose the correct physical boundary conditions which are necessary to complete the specification of the initial boundary value problem given by equation (1) in the region given by equation (18). In typical calculations there are two types of boundaries. The upper boundary, y=0, is a free surface along which the appropriate conditions are $\tau_{12}=\tau_{22}=0$. Since the scheme is a centered scheme we must calculate the other variables u, v, τ_{11} by some other means. We calculate these variables by extrapolation based on characteristic variables.

Based on a one dimensional analysis (i.e. neglecting x derivatives) the quantity

$$R_1 = \sqrt{\rho\mu}\ u + \tau_{12} \tag{20}$$

is convected toward the boundary with velocity C_s,

$$R_2 = \sqrt{(\lambda + 2\mu)\rho}\ v + \tau_{22} \tag{21}$$

is convected toward the boundary with velocity C_p and

$$R_3 = (\lambda + 2\mu)\tau_{11} - \mu\tau_{22} \tag{22}$$

moves with zero normal velocity. We specify R_1, R_2, R_3 by the values obtained from the interior scheme with the boundary fluxes extrapolated using equation (19). This combined with the free surface conditions $\tau_{22}=\tau_{12}=0$ enables us to obtain all of the dependent variables. (For problems with a surface source, the above procedure is carried out with τ_{22} and τ_{12} equal to the prescribed forces). The use of one-dimensional characteristic variables was shown in (Gottlieb et. al., 1982) to enhance the stability of the boundary treatment. we have found that the specification of the zero characteristic R_3 is necessary when the Poisson ratio is large or when the material is

highly anisotropic.

In addition to the free surface there are three other boundaries; $x=0$, $x=L_1$ and $y=-L_2$. These are all artificial boundaries and appropriate absorbing boundary condition must be imposed. We use the one-dimensional characteristics given by equations (20-22) (or the analogue obtained by neglecting y derivatives when the boundary is the line x = constant) and impose the boundary condition that the incoming characteristic variable is zero. This characteristic condition is the same as the viscous boundary condition proposed by (Lysmer and Kuhlemeyer, 1969). Using the first order system (equation (1)) it becomes a Dirichlet condition which can be implemented very easily. These conditions are exact for compressional and shear waves impinging normally on the boundary. Since they are based on one-dimensional characteristics they do not absorb Rayleigh waves. The Rayleigh wave reflection can be ameliorated by burying the source or by making a subsidiary calculation of the free space problem with just the upper layer of the model and subtracting that solution from the computed solution. We are investigating more satisfactory solutions to this problem.

In (Clayton and Engquist, 1977) boundary conditions based on paraxial approximations to elastic waves were introduced. The first order condition in (Clayton and Engquist, 1977) is equivalent to the characteristic condition in one dimension but differs in two dimension because of the replacement of the shear stress by a displacement. The higher order paraxial boundary conditions are theoretically more effective absorbers as the waves deviate from normal incidence. (Cohen et. al., 1981) have found that these higher order boundary condi-

tions are not significantly more effective than the viscous boundary conditions and we have not found pernicious reflections in the examples considered in the next section. None of these boundary conditions accounts for the cylindrical decay of the compressional and shear waves. A family of boundary conditions which account for the cylindrical decay of acoustic waves is described in (Bayliss and Turkel, 1980).

NUMERICAL RESULTS

In this section we present some numerical examples which illustrate the advantages of the finite difference scheme described above. In the first example we consider the Lamb problem for a surface line source. Specifically we take

$$\tau_{22} = f(t)\delta(x) \tag{23}$$

on the free surface. The functional form of the source is

$$f(t) = -\frac{4}{\sigma^2}\left(e^{-2(t-t_s)^2/\sigma^2} - e^{-2(t_s/\sigma))^2}\right)(t-t_s). \tag{24}$$

The material properties were chosen so that the compressional speed was 7000 ft./sec., the shear speed was 4000 ft./sec. and the density was taken as 1.0. The parameters of the source were σ = .017 sec and the time shift (t_s) was 0.285 sec. The spatial delta function was modelled by the discrete function which is zero except at the location of the source where it is equal to 1/h (h is the grid size).

The coupled wave equation for the elastic displacements can also be considered as coupled wave equations for the elastic velocities provided we use a source that is the derivative of equation (24). Using the parameters described above the peak frequency of the derivative of the source is approximately 26.5 Hertz. We compared the solution with the exact solution (Miklowitz, 1978) and with solutions obtained from the (2-2) scheme (Kelly et. al., 1976). A second order accurate implementation of the free surface condtion was used (B. Nair private communication).

In Figures 1a and 1b we compare the horizontal velocity u at a receiver location of 100 ft. from the source. We compare the exact solution with results from the finite difference calculations using a

mesh size of 10 ft. It is apparent that the (2-4) scheme is more accurate. In refining the grid we found that the (2-2) scheme with 5 ft. spacing gave a solution that was comparable to the (2-4) scheme with 10 ft. spacing. This is exhibited in Figure 1c.

In Figure 2 we demonstrate the effect of increasing the Poisson ratio. The parameters are the same except that the compressional velocity is increased to 16000 ft./sec. giving a Poisson ratio of 0.4667. The results demonstrate that the (2-4) scheme is stable and that there is little loss in accuracy as the Poisson ratio increases. The implementation of the free surface condition which we used with the (2-2) scheme was not stable at this Poisson ratio. We did not test the implementation of (Ilan and Loewenthal, 1976) which appears to be more stable at higher Poisson ratios.

We next demonstrate the accuracy of the numerical scheme on body waves reflected from an interface. We consider a surface source of the above form and an interface 400 ft. below the free surface. At the interface the velocities jump to 12000 ft./sec. (compressional) and 8000 ft./sec. (shear). The density is kept constant.

We have found that for a given source and mesh size the Rayleigh waves tend to be significantly less accurate than the body waves. There are several reasons for this. The Rayleigh waves tend to be a higher order derivative than the body waves (see Miklowitz, 1978) and thus there is more energy in the higher frequencies. In addition, the Rayleigh wave profiles are steep in the normal direction thus requiring more resolution. The accuracy is also sensitive to the treatment of the free surface condition. Finally Rayleigh waves propagate parallel to the grid and many schemes tend to be least accurate for waves that propagate parallel to the grid.

For some problems in seismology the reflected body waves are more important than the Rayleigh waves. In order to asses the accuracy of the two schemes on the body waves we compared solutions on the free surface obtained with both numerical schemes. The time intervals were chosen so as not to include the Rayleigh wave. Mode converted arrivals and multiple reflections off the free surface did occur during the chosen time interval. In order to enhance the separation of the arrivals, the duration of the source pulse was reduced by setting σ = .0125 sec.

The programs were run with grid refinement until no further changes were visible. It was found that the (2-4) scheme with a mesh size of 5 ft. could be taken as the exact solution. A comparision for the horizontal velocity u at a receiver location of 100 ft. is shown in Figures 3a and 3b. In Figure 3a we compare the solution obtained with the (2-4) scheme with a mesh size of 5 ft. to the solution obtained with the (2-4) scheme and a mesh size of 7.5 ft. It is apparent that the solutions agree closely, with the major source of errors being a slight amplitude attenuation in the later arrivals. In contrast, we compare in Figure 3b the (2-2) scheme with a mesh size of 7.5 ft. to the (2-4) scheme with a mesh size of 5.0 ft. The second order solution is quite inaccurate, exhibiting both amplitude errors and additional lobes characteristic of numerical dispersion.

In order to assess the properties of the two schemes for waves propagating at wider angles to the grid we make the same comparison in Figures 4a and 4b for a receiver location at 800 ft. The same conclusion can be drawn. In Figure 4c we compare the (2-4) scheme and the (2-2) scheme both with mesh sizes of 5 ft. It can be inferred that the second order scheme with a mesh size of 5 ft. is comparable

in accuracy to the fourth order scheme with a mesh size of 7.5 ft.

In summary the results for this model demonstrate that both schemes perform worst for waves propagating nearly parallel to the grid. The (2-4) scheme is less anisotropic. For models of this size and sources of the form of equation (24) body waves require roughly two-thirds less resolution in each dimension with the (2-4) scheme than with the (2-2) scheme for comparable accuracy. Rayleigh waves require roughly half the resolution. The accuracy and stability of the (2-4) scheme does not appear to be sensitive to Poisson ratio. We have obtained results for problems with curved interfaces, including models which allow caustic formation. The conclusions for these cases are similiar to those already presented.

In our final example we consider the problem of Rayleigh wave scattering from a fluid. The geometry is shown in Figure 5. For simplicity, the Rayleigh wave is generated by a surface source in the elastic region. The acoustic fluid is treated by setting the shear modulus to zero and differencing across the interface. The free surface condition is replaced by a pressure release boundary condition over the fluid.

This problem is designed to demonstrate that the scheme is accurate and stable at a fluid-elastic interface. We refer to (Stephen, 1983) for a discussion of the numerical difficulties that can be expected at a fluid-elastic interface. The source function is the same as for the first example. In Figure 6 we plot a snapshot of the vertical velocity at t = 0.35 sec. The impinging Rayleigh wave generates an interfacial wave which travels along the fluid-elastic interface and a wave which travels throught the fluid. The slow velocity of the interfacial wave governs the resolution requirements of the

problem. Body waves are generated at the interface and propagate away from the fluid.

In order to assess the accuracy of the computation, we examine time traces of the horizontal velocity for different grids. We choose a receiver location at 1500 ft. so that interference by the slow interfacial wave can be seen. In Figures 7a and 7b the solution with grid sizes of 4 and 6 ft. are compared with the solution obtained with a grid size of 2.5 ft. The solution does not change if the grid is refined further. It is apparent that the solution converges as the grid is refined. We have not run this case with the (2-2) scheme but based on the results presented above we expect that the (2-2) scheme would require substantially more resolution to obtain a solution of comparable accuracy. Considerably more resolution is required than for the corresponding Lamb problem. This is primarily because of the slow velocity of the interfacial wave. The computations were stable provided the CFL number (see above) was reduced to 0.5.

This computation, together with others that we have made, demonstrates that there are no stability problems in applying the scheme at a fluid-elastic interface. The change to a pressure release boundary condition over the fluid provides a further test of the robustness of the scheme. We have repeated this computation with the Poisson ratio in the elastic region increased to 0.4667 and again no instabilities were found. Although the resolution requirements in this problem are governed by a slow interfacial wave, we have examined body waves reflected from a fluid-elastic interface and found no degradation in accuracy compared to a corresponding elastic-elastic interface. The numerical scheme provides a simple and robust method to compute scattering from curved fluid-elastic interfaces.

CONCLUSION

The numerical results presented here clearly demonstrate the improvements in accuracy that can be obtained from the use of fourth order accurate differences to compute elastic waves. We have tested the scheme on a variety of problems involving wave scattering from curved interfaces, fluid-elastic interfaces and regions of high Poisson ratio. The results presented here are representative of the improvements due to the fourth order differencing.

The scheme presented here permits an accurate and robust implementation of the free surface condition. For body waves, with sources of the same form as equation (24), we have found that from 13-16 points per shear wavelength, based on the peak frequency of the derivative of the source, is required for reasonable accuracy. This is for models approximately 20-30 wavelengths in size. Larger models require more resolution per wavelength. This is shown mathematically by (Kreiss and Oliger, 1973) and demonstrated numerically by (Stephen, 1982). Resolution requirements grow at a much slower rate with fourth order differencing (Kreiss and Oliger, 1973). Considerably more resolution is required to approximate Rayleigh waves than body waves.

The scheme is suitable for vector computers. A sustained rate of 56 MFLOPS (Million Floating Point Operations Per Second) can be obtained on a Cray 1-S. On a Cray XMP/48 using only one processor a rate of 83 MFLOPS can be obtained. Using all four processors rather than one a sustained rate of 328 MFLOPS can be obtained. The improvement in using four processors rather than one is 3.95. (The authors are grateful to Michael Booth of Cray Research Inc. for assistance in adapting the program to run on multi-processors). Schemes based on operator splitting are particularly well suited to multi-processing.

For example during an x update each line y=constant can be given to a separate processor. A further discussion of this can be found in (Schenck et. al., 1985). A benchmark problem with a grid of 701x301 and run for 2560 timesteps, required 660 seconds on the Cray 1-S and 116 seconds on the XMP/48. (This run and all of the other cases discussed here used an expanding grid as suggested by (Boore, 1972)).

There are applications where the explicit imposition of interface conditions may be more efficient than the heterogeneous formulation. For example, models with localized regions of low velocity would require significant oversampling unless different grids were used in different regions. The scheme described here appears to be applicable to a wide variety of problems of seismological interest. It could also be used with the explicit imposition of interface conditions (homogeneous formulation) provided interface conditions of sufficient accuracy were imposed.

REFERENCES

Alford, R. M., K.R. Kelly and D.M. Boore (1974). Accuracy of finite difference modeling of the acoustic wave equation. Geophysics, 39, pp. 834-842.

Bayliss, A. and E. Turkel (1980). Radiation boundary conditions for wave-like equations. Comm. Pure and Applied Math, 33 pp. 707-726.

Boore, D.M. (1972). Finite difference methods for seismic waves. In Methods in Computational Physics, Academic Press, 11, pp. 1-37.

Clayton, R. and B. Engquist. (1977). Absorbing boundary conditions for acoustic and elastic wave equations. Bull. Seism. Soc. Am., 67, pp. 1529-1541.

Clifton, R.J. (1967). A difference method for plane problems in elasticity. Quart. Appl. Math., 25, pp. 97-116.

Cohen, M.F., T.J.R. Hughes,. and P.C. Jennings (1981). A comparison of paraxial and viscous silent boundary methods in finite element analysis. Joint ASME/ASCE Mechanincs Converence, University of Colorodo, pp. 67-80.

Emerman, S.H., W. Schmidt and R.A. Stephen (1982). An implicit finite-difference formulation of the elastic wave equation. Geophysics, 47, pp. 1521-1526.

Gottlieb, D., M.D. Gunzberger and E. Turkel. (1982). On numerical boundary treatment for hyperbolic systems. SIAM J. Numer. Anal. 19, pp. 671-682.

Gottlieb, D. and E. Turkel (1976). Dissipative two-four methods for time-dependent problems. Math. Comp., 30, pp. 703-723.

Ilan, A. and D. Loewenthal (1976). Instability of finite difference schemes due to boundary conditions in elastic media. Geophysical Prospecting, 24, pp. 431-453.

Kelly, K.R., R.W. Ward, S. Treitel, and R.M. Alford (1976). Synthetic seismograms: A finite difference approach. Geophysics, 41, pp. 2-27.

Kosloff, D.D., M. Reshef and D. Lowenthal (1984). Elastic wave calculations by the Fourier method. Bull. Seism. Soc. Am., 74, pp. 875-891.

Kreiss, H. O. and J. Oliger (1972). Comparision of accurate methods for the integration of hyperbolic systems. Tellus, 24, pp. 199-215.

Lysmer, J. and R.L. Kuhlemeyer (1969). Finite dynamic model for infinite media. Journal of the Engineering Mechanics Division, ASCE, 101, pp.859-877.

Maestrello, L., A. Bayliss, and E. Turkel (1981). On the interaction of a sound pulse with the shear layer of an axisymmetric jet. Journal of Sound and Vibration, 74, pp. 281-301.

Miklowitz, J. (1978). The theory of elastic waves and waveguides. North Holland Publishing Co.

Oliger, J. (1976). Hybrid difference methods for the initial boundary-value problem for hyperbolic equations. Math. Comp., 30, pp. 724-738.

Schenck, P.B., D. Austin, S.L. Squires, J. Lehmann, D. Mizell, and K. Wallgren (1985). Parallel Processor Programs in the Federal Government. Computer 18, pp.43-56.

Stephen, R. A. (1983). A comparison of finite difference and reflectivity seismograms for marine models. Geophys. J. R. astr. Soc. 72, pp. 39-58.

Strang, W.,G. (1968). On the construction and comparison of difference schemes. SIAM Journal of Numerical Analysis, 5, pp. 506-517.

Turkel, E. (1974). Phase error and stability of second order methods for hyperbolic problems. I. J. Comp. Phys, 15, pp. 226-250.

FIGURE CAPTIONS

1.a Comparison of exact solution to the Lamb problem (solid curve) to solution obtained with (2-4) scheme using a grid size of 10 ft. (dotted curve). Horizontal velocity (u) plotted at a receiver location 100 ft. from the source.

1.b Comparison of exact solution to the Lamb problem (solid curve) to solution obtained with (2-2) scheme using a grid size of 10 ft. (dotted curve). Horizontal velocity (u) plotted at a receiver location 100 ft. from the source.

1.c Comparison of exact solution to the Lamb problem (solid curve) to solution obtained with (2-2) scheme using a grid size of 5 ft. (dotted curve). Horizontal velocity (u) plotted at a receiver location 100 ft. from the source.

2 Comparison of exact solution to the Lamb problem (solid curve) to solution obtained with (2-4) scheme using a grid size of 10 ft. (dotted curve). Horizontal velocity (u) plotted at a receiver location 100 ft. from the source. Poisson ratio is 0.4667.

3.a Comparison of reflected body waves. Solid curve is (2-4) scheme using a mesh size of 5 ft. Dotted curve is obtained from (2-4) scheme using a mesh size of 7.5 ft. Horizontal velocity (u) plotted at a receiver location 100 ft. from the source.

3.b Comparison of reflected body waves. Solid curve is (2-4) scheme using a mesh size of 5 ft. Dotted curve is obtained from (2-2) scheme using a mesh size of 7.5 ft. Horizontal velocity (u) plotted at a receiver location 100 ft. from the source.

4.a Comparison of reflected body waves. Solid curve is (2-4) scheme using a mesh size of 5 ft. Dotted curve is obtained from (2-4) scheme using a mesh size of 7.5 ft. Horizontal velocity (u) plotted at a receiver location 800 ft. from the source.

4.b Comparison of reflected body waves. Solid curve is (2-4) scheme using a mesh size of 5 ft. Dotted curve is obtained from (2-2) scheme using a mesh size of 7.5 ft. Horizontal velocity (u) plotted at a receiver location 800 ft. from the source.

4.c Comparison of reflected body waves. Solid curve is (2-4) scheme using a mesh size of 5 ft. Dotted curve is obtained from (2-2) scheme using a mesh size of 5 ft. Horizontal velocity (u) plotted at a receiver location 800 ft. from the source.

5 Model for problem of Rayleigh wave scattering from fluid.

6 Snapshot of vertical velocity (v) obtained for problem of Rayleigh wave scattered from fluid. Time is 0.35 sec

7.a Comparison of solutions obtained for problem of Rayleigh wave scattering from fluid. Solid curve is obtained with grid size of 2.5 ft. Dotted curve had grid size of 6 ft. Horizontal

velocity (u) plotted at receiver location 1500 ft. from source.

7.b Comparison of solutions obtained for problem of Rayleigh wave scattering from fluid. Solid curve is obtained with grid size of 2.5 ft. Dotted curve had grid size of 4 ft. Horizontal velocity (u) plotted at receiver location 1500 ft. from source.

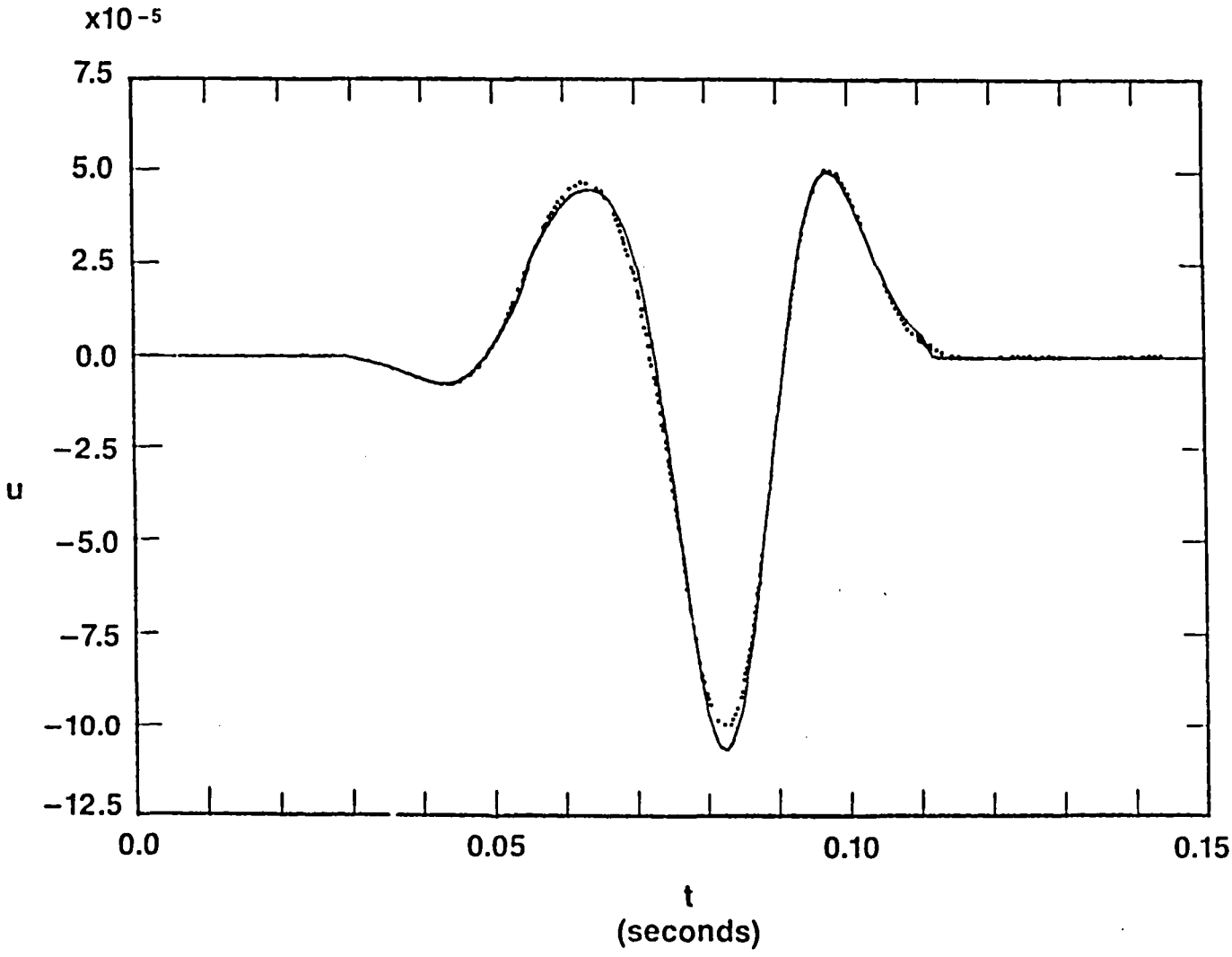

Figure 1.a

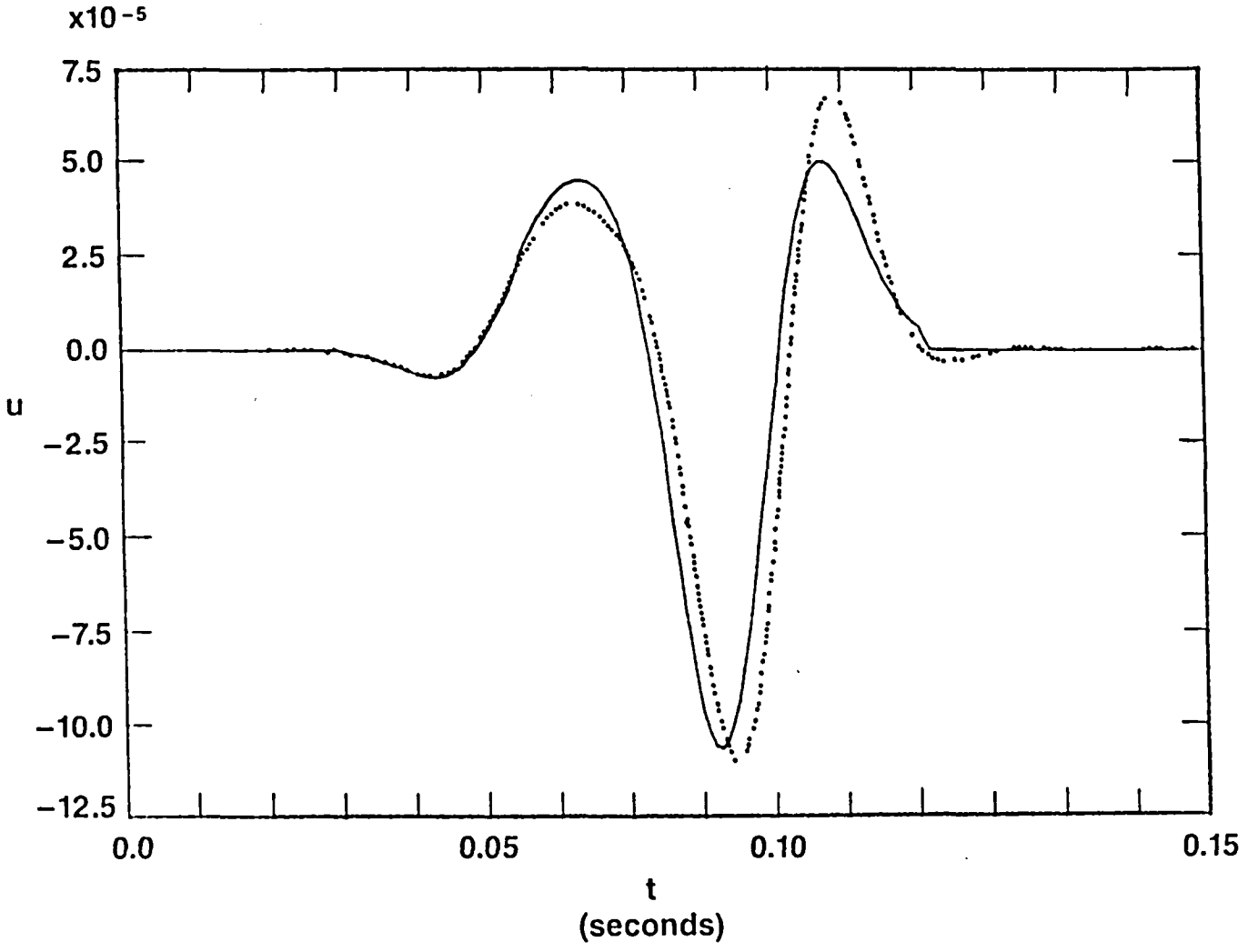

Figure 1.b

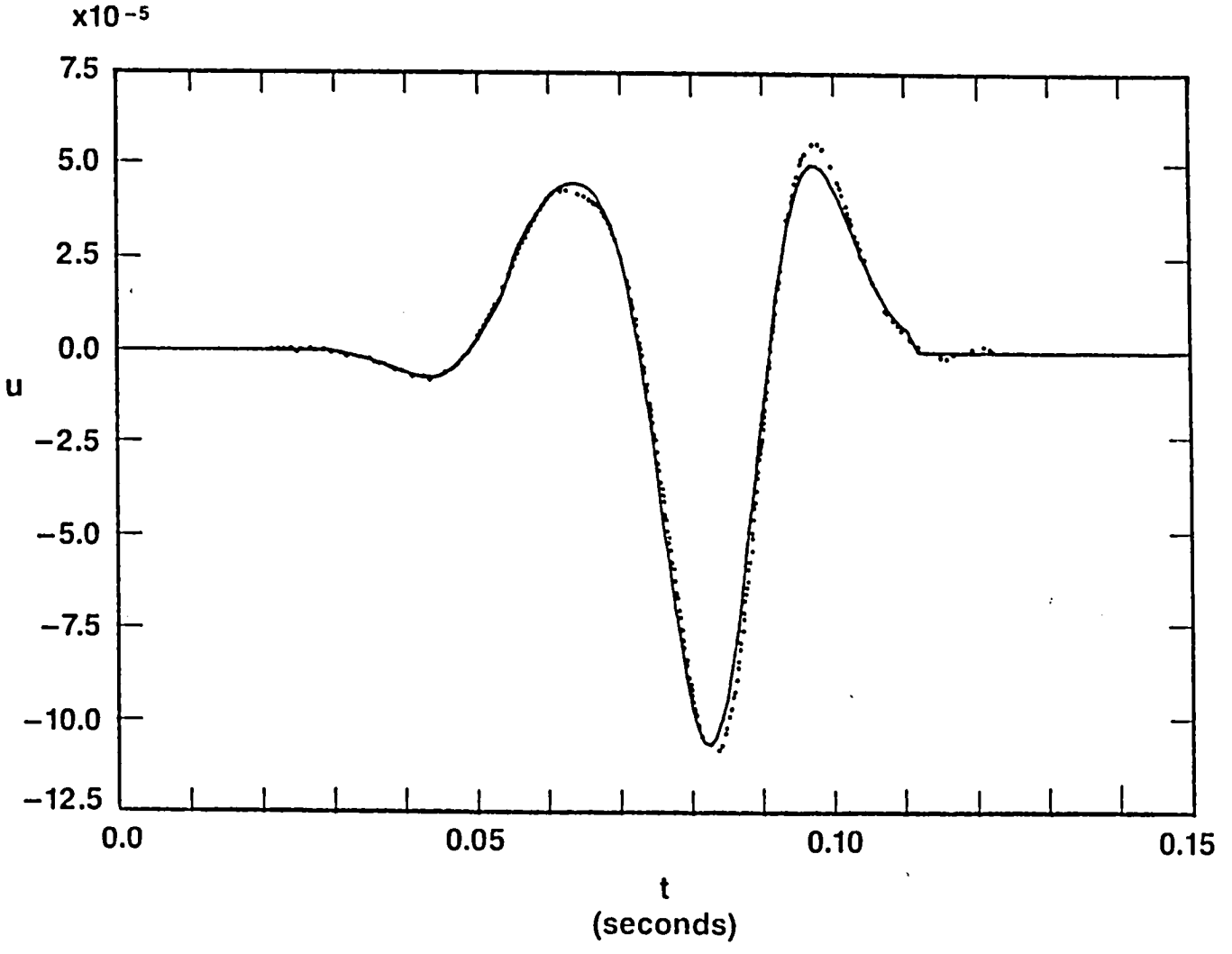

Figure 1.c

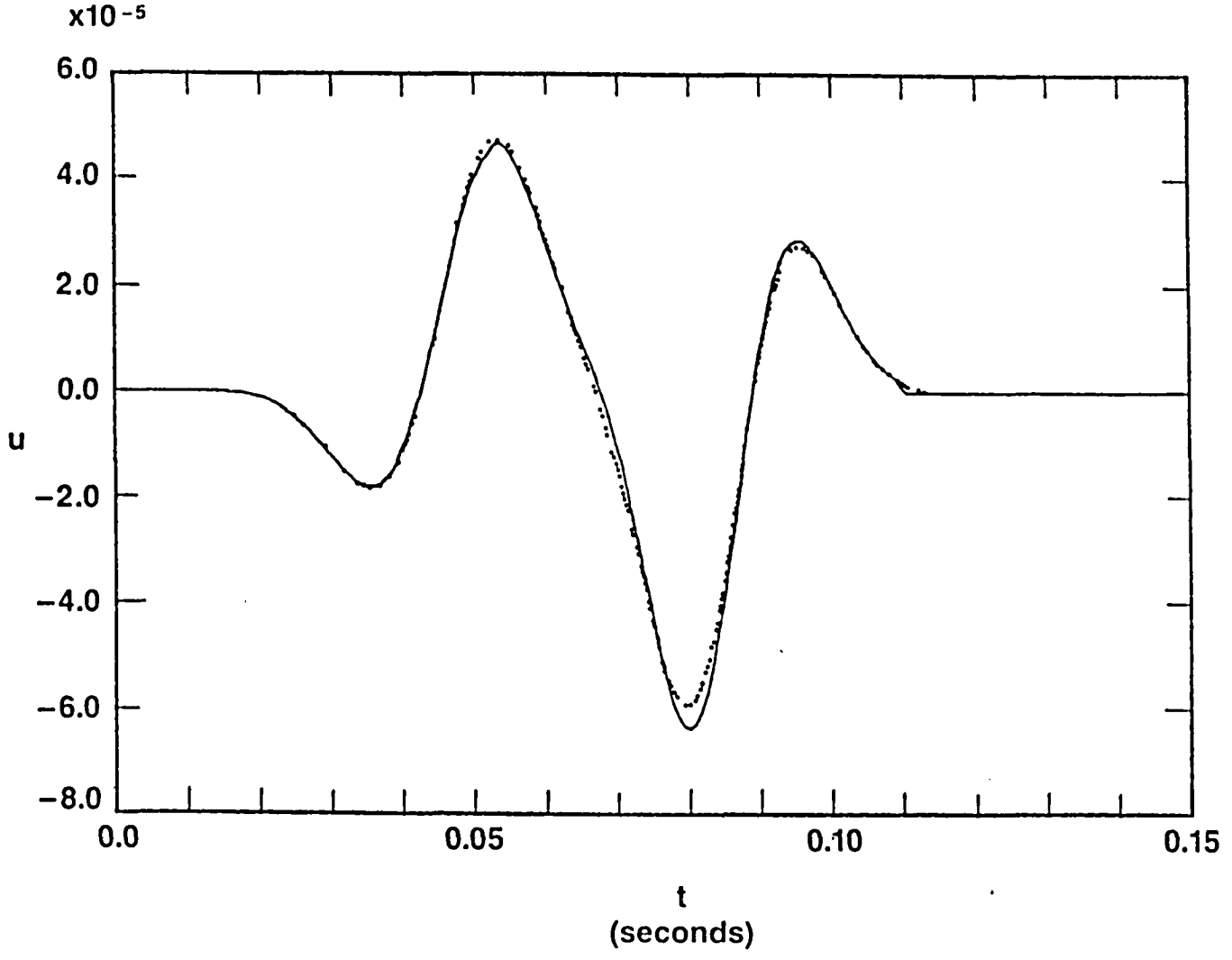

Figure 2

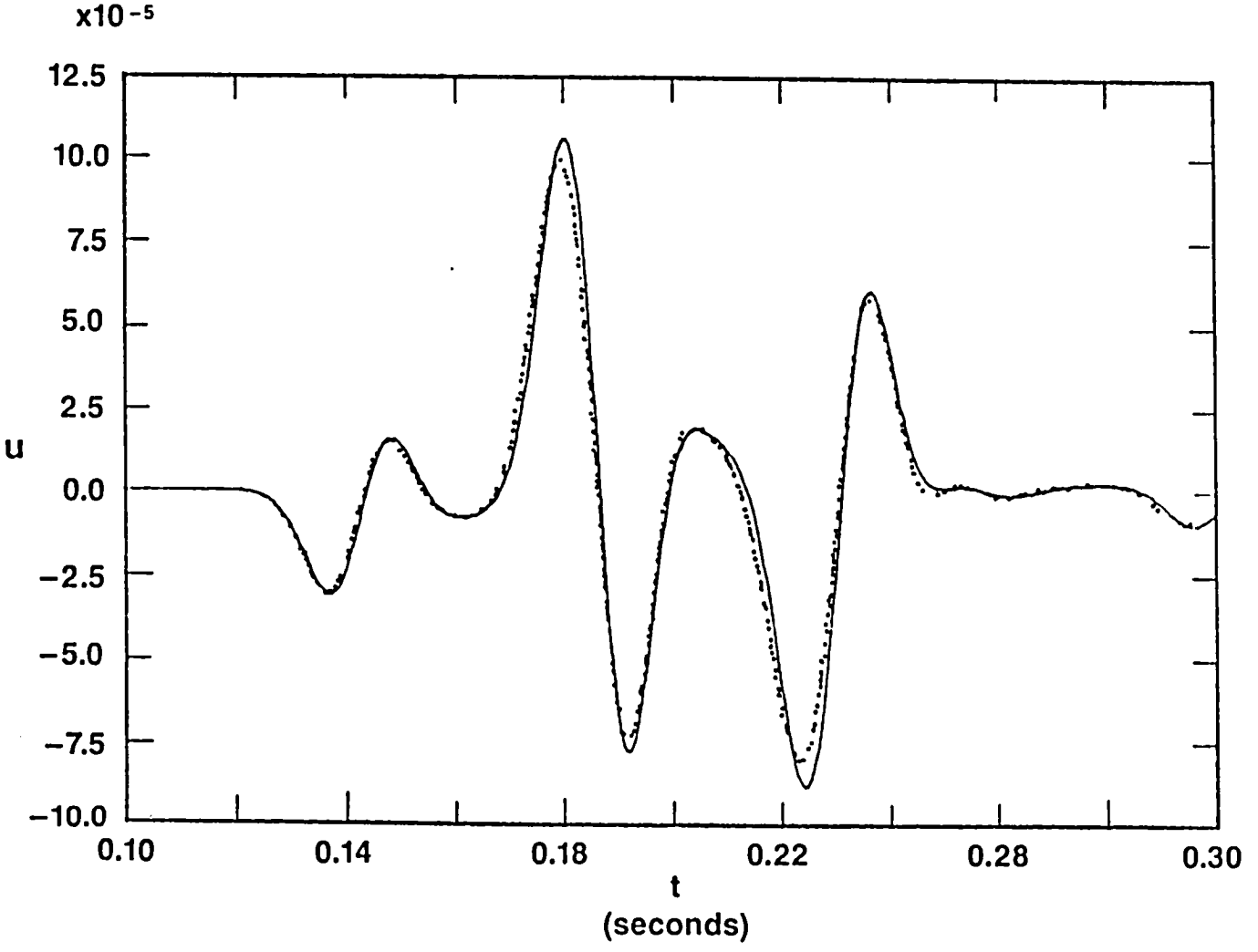
x10 -5
12.5
10.0
7.5
5.0
2.5
0.0
-2.5
-5.0
-7.5
-10.0
u
0.10
0.14
0.18
0.22
0.28
0.30
t
(seconds)

Figure 3.a

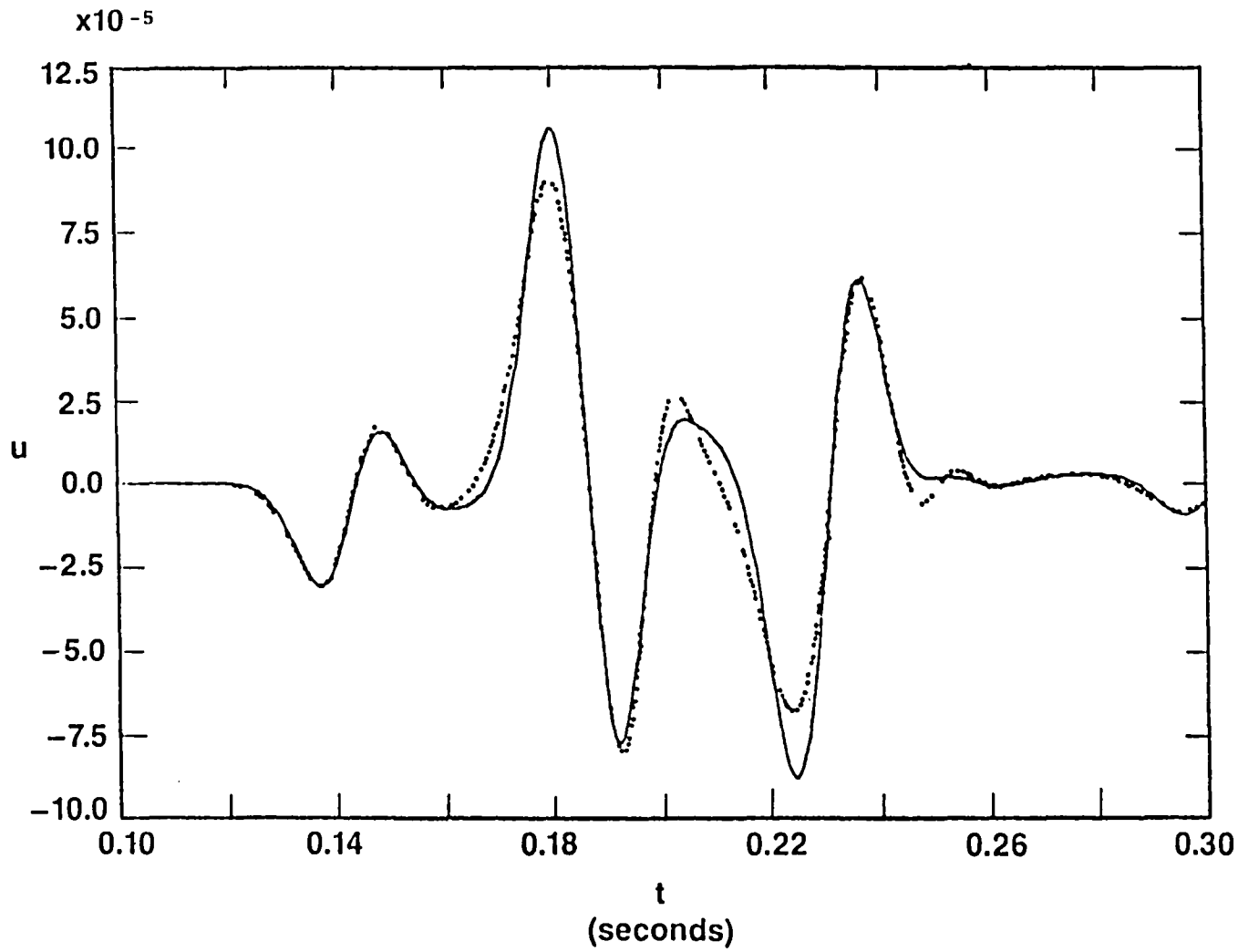
x10 -5
12.5
10.0
7.5
5.0
2.5
u
0.0
-2.5
-5.0
-7.5
-10.0
0.10
0.14
0.18
0.22
0.26
0.30
t
(seconds)

Figure 3.b

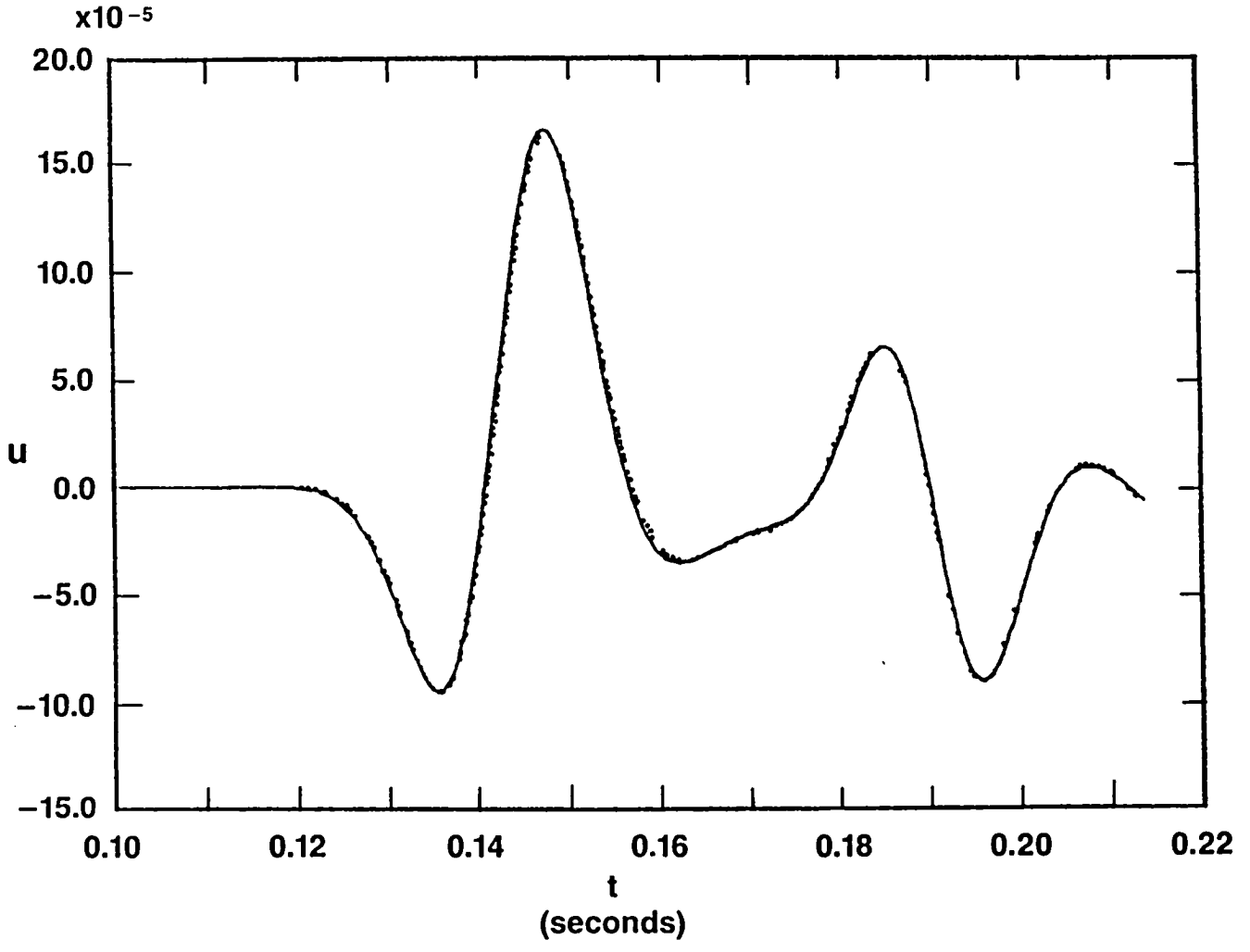
x10 -5
20.0
15.0
10.0
5.0
u
0.0
-5.0
-10.0
-15.0
0.10
0.12
0.14
0.16
0.18
0.20
0.22
t
(seconds)

Figure 4.a

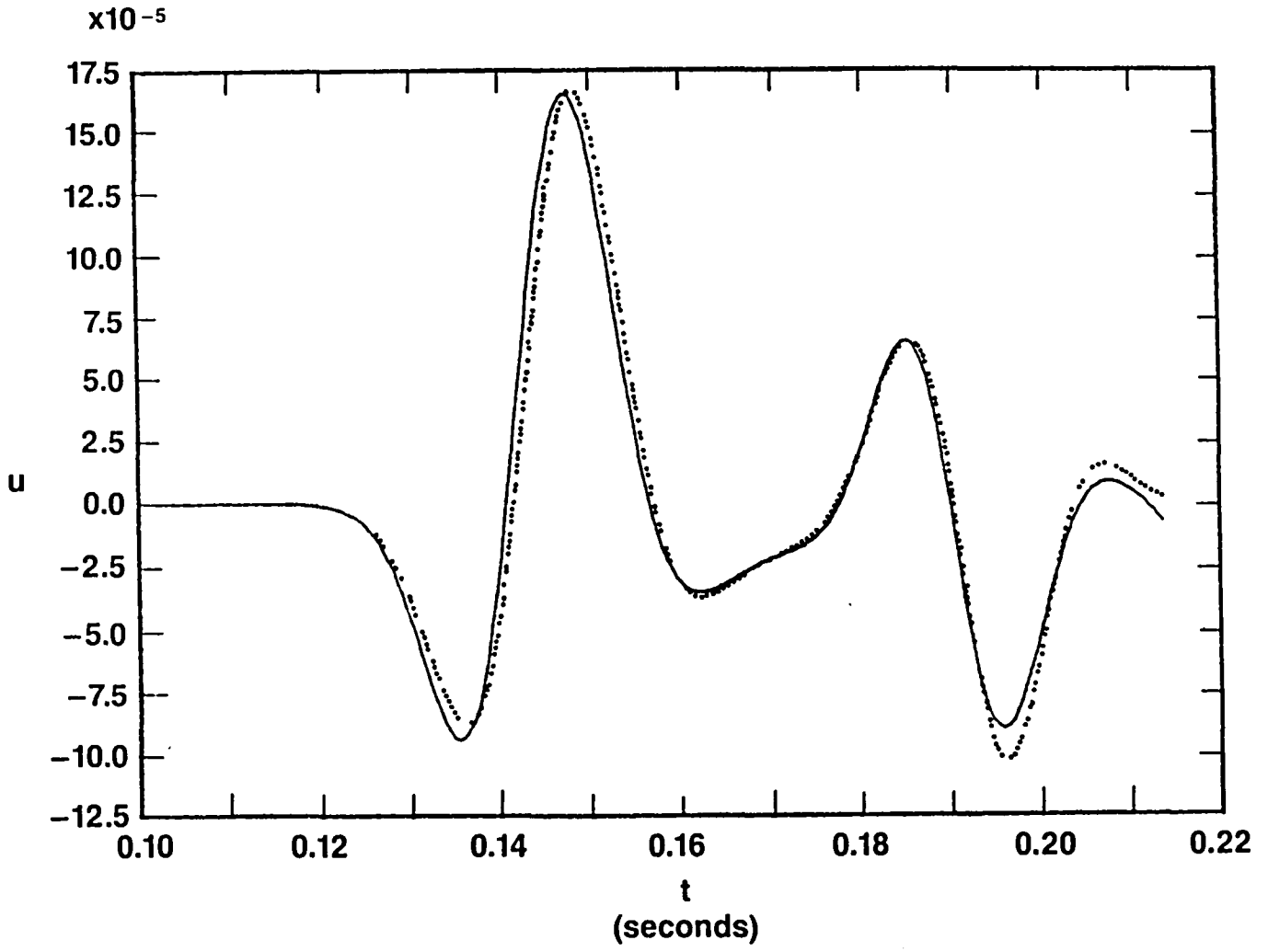
x10 -5
17.5
15.0
12.5
10.0
7.5
5.0
2.5
0.0
-2.5
-5.0
-7.5
-10.0
-12.5
u
0.10
0.12
0.14
0.16
0.18
0.20
0.22
t
(seconds)

Figure 4.b

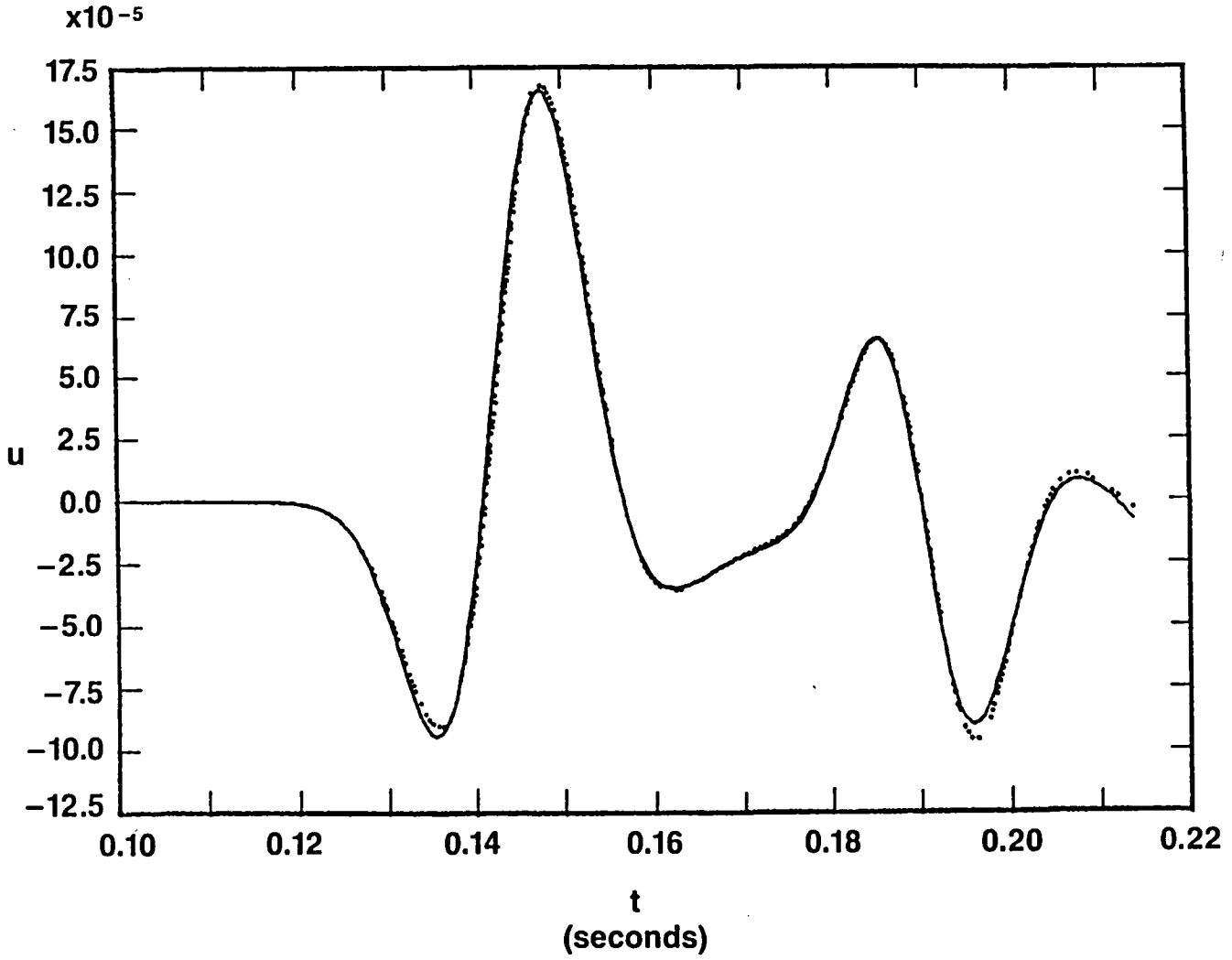
x10-5
17.5
15.0
12.5
10.0
7.5
5.0
2.5
0.0
-2.5
-5.0
-7.5
-10.0
-12.5
u
0.10
0.12
0.14
0.16
0.18
0.20
0.22
t
(seconds)

Figure 4.c

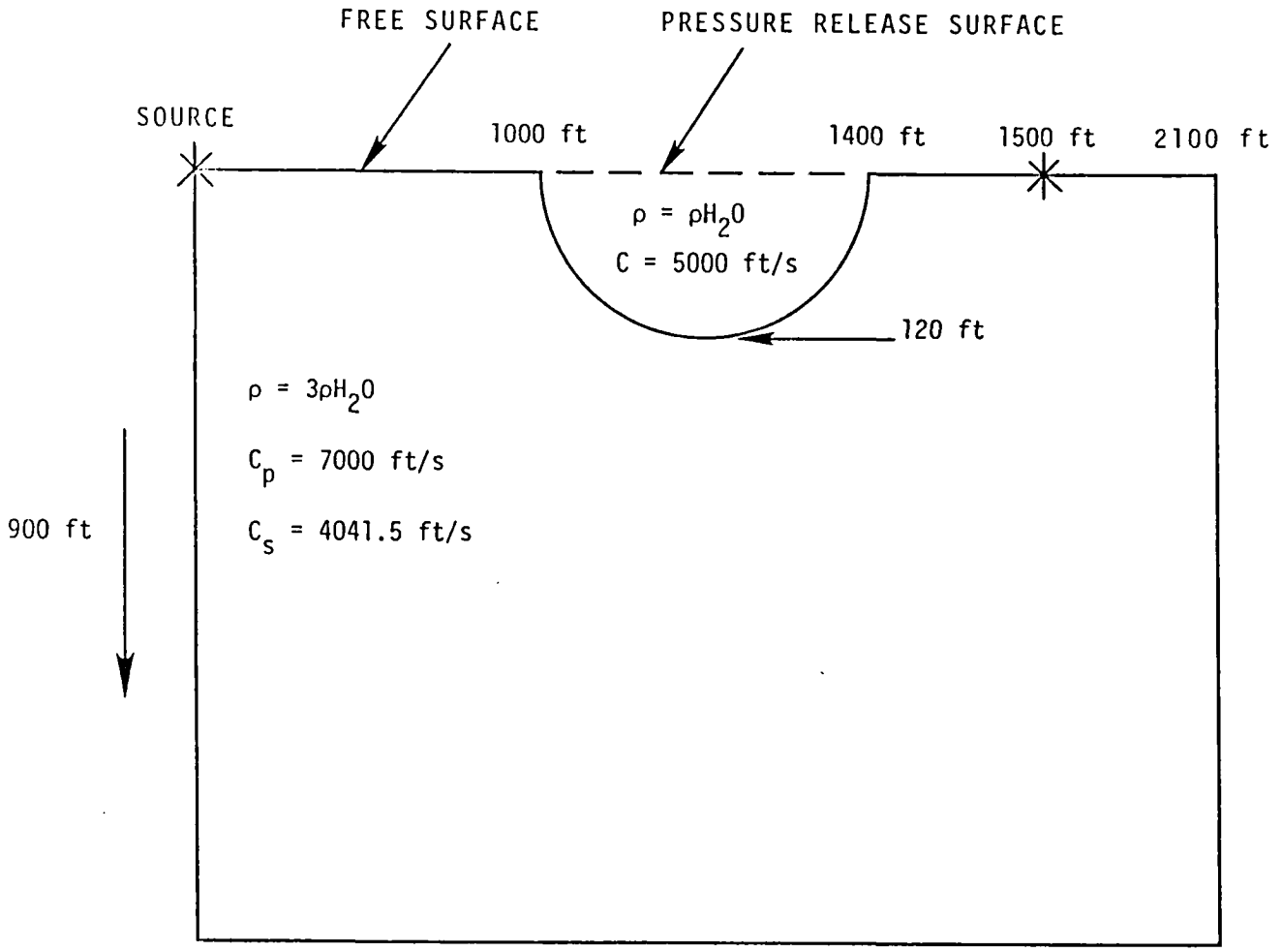
FREE SURFACE
PRESSURE RELEASE SURFACE
SOURCE
1000 ft
1400 ft
1500 ft
2100 ft
ρ = ρH2O
C = 5000 ft/s
120 ft
ρ = 3ρH2O
Cp = 7000 ft/s
Cs = 4041.5 ft/s
900 ft

Figure 5

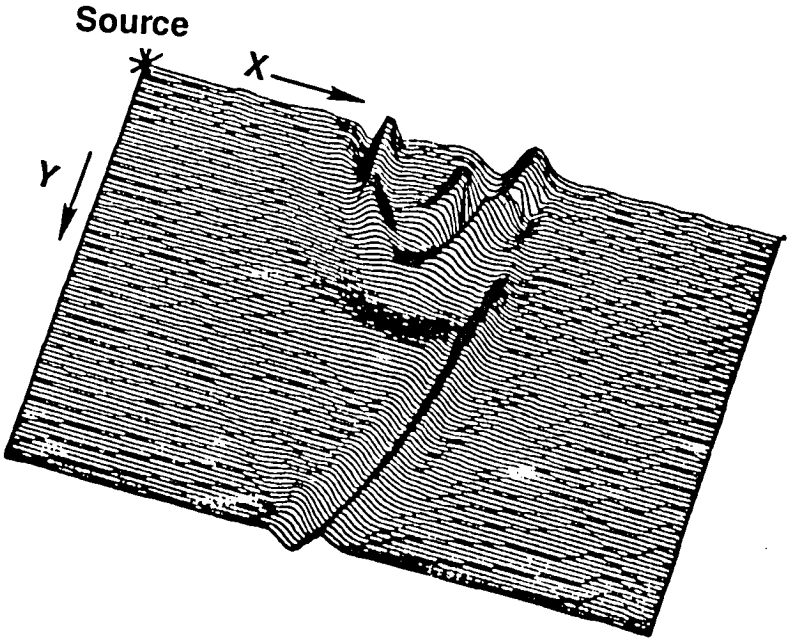

Figure 6

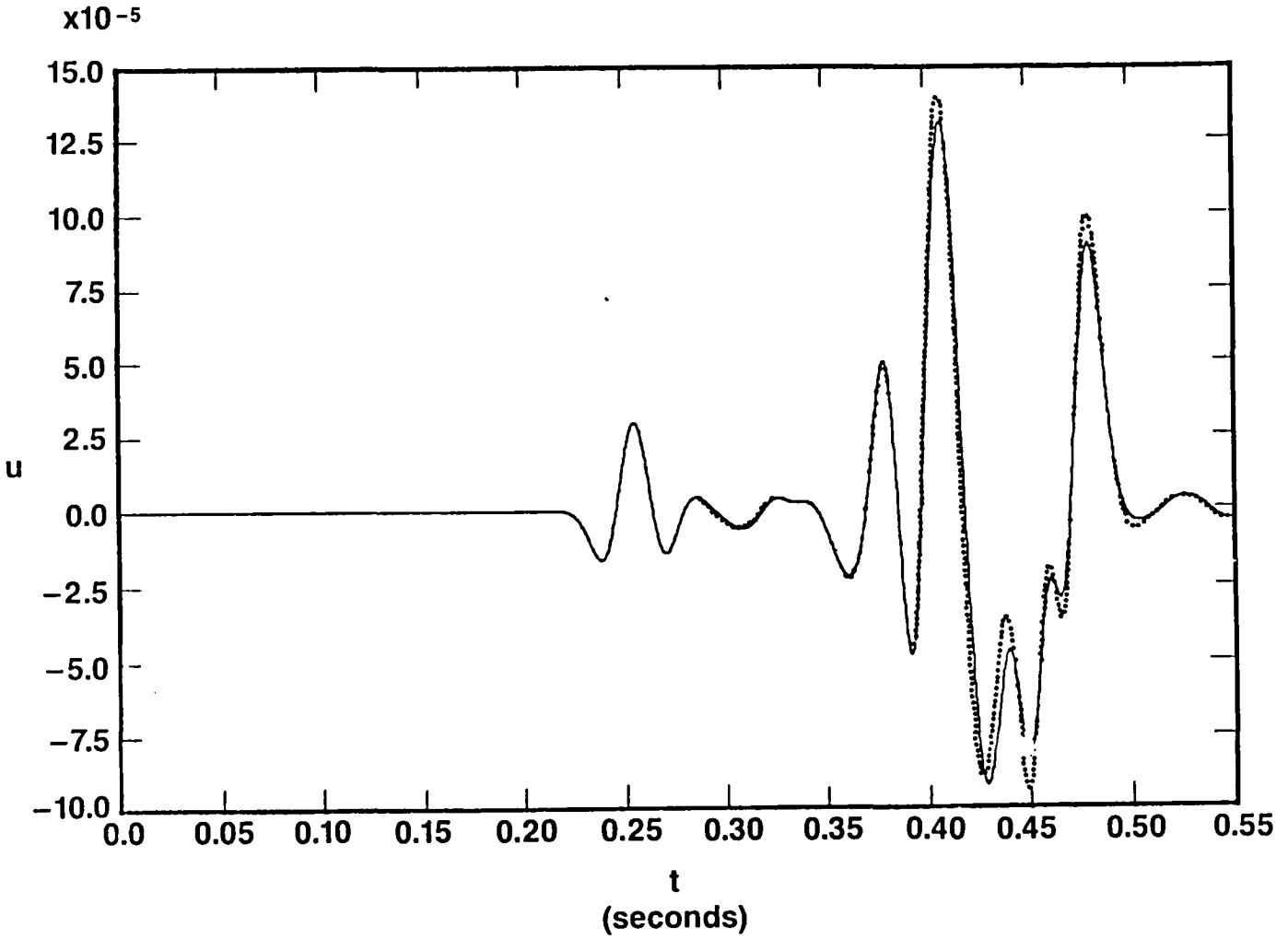
x10-5
15.0
12.5
10.0
7.5
5.0
2.5
0.0
-2.5
-5.0
-7.5
-10.0
u
0.0
0.05
0.10
0.15
0.20
0.25
0.30
0.35
0.40
0.45
0.50
0.55
t
(seconds)

Figure 7.a

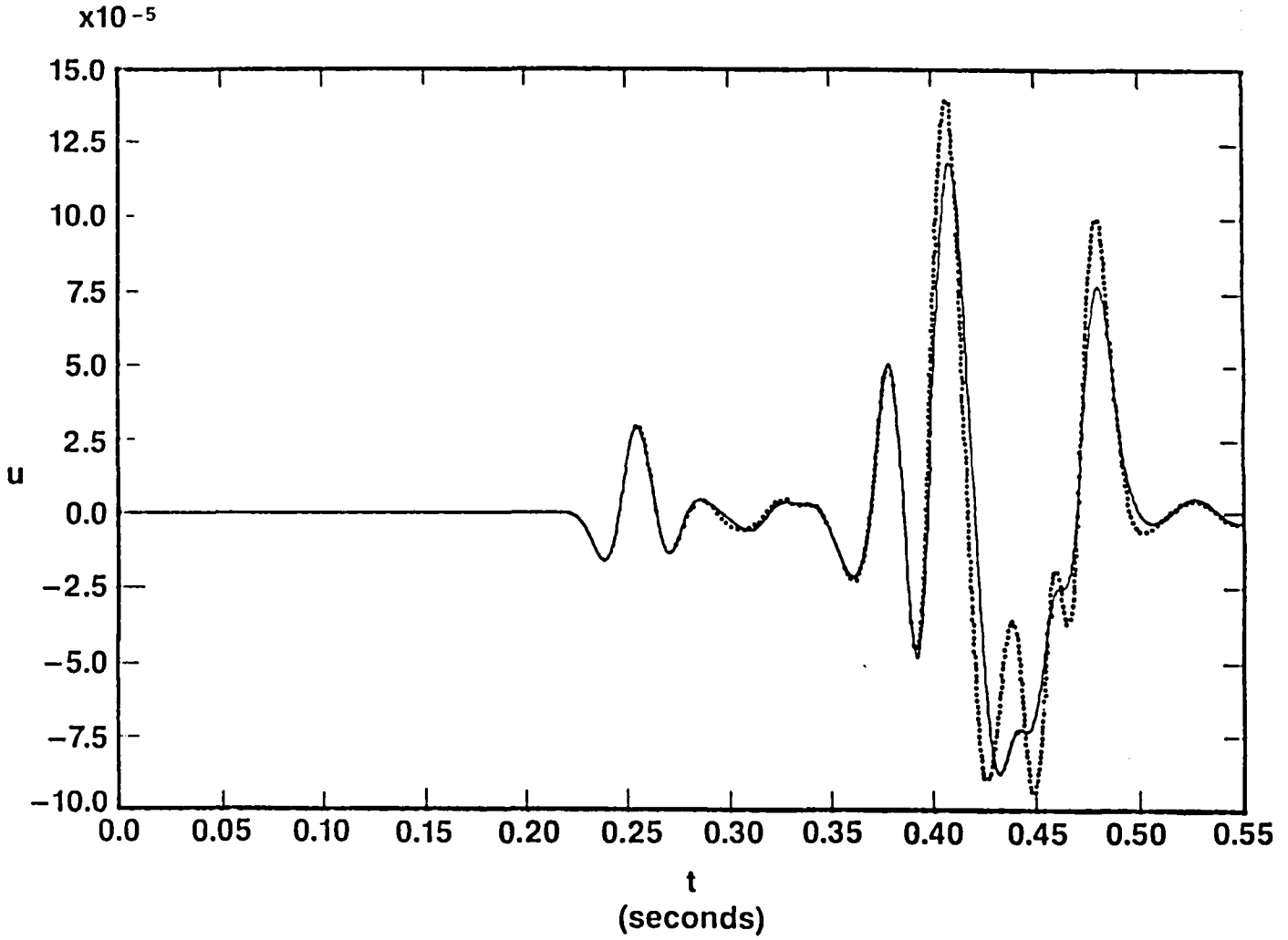
x10 -5
15.0
12.5
10.0
7.5
5.0
2.5
0.0
−2.5
−5.0
−7.5
−10.0
u
0.0
0.05
0.10
0.15
0.20
0.25
0.30
0.35
0.40
0.45
0.50
0.55
t
(seconds)

Figure 7.b

1. Report No. NASA CR-178089 ICASE Report No. 86-21	2. Government Accession No.	3. Recipient's Catalog No.
4. Title and Subtitle A FOURTH ORDER ACCURATE FINITE DIFFERENCE SCHEME FOR THE COMPUTATION OF ELASTIC WAVES		5. Report Date April 1986 6. Performing Organization Code
7. Author(s) A. Bayliss, K. E. Jordan, B. J. LeMesurier, E. Turkel		8. Performing Organization Report No. 86-21
9. Performing Organization Name and Address Institute for Computer Applications in Science and Engineering Mail Stop 132C, NASA Langley Research Center Hampton, VA 23665-5225		10. Work Unit No. 11. Contract or Grant No. NAS1-17070, NAS1-18107
12. Sponsoring Agency Name and Address National Aeronautics and Space Administration Washington, D.C. 20546		13. Type of Report and Period Covered Contractor Report 14. Sponsoring Agency Code 505-31-83-01

15. Supplementary Notes

Langley Technical Monitor:
J. C. South

Submitted to Bulletin of the Seismological Society of America

Final Report

16. Abstract

A finite difference for elastic waves is introduced. The model is based on the first order system of equations for the velocities and stresses. The differencing is fourth order accurate on the spatial derivatives and second order accurate in time. The model is tested on a series of examples including the Lamb problem, scattering from a plane interfaces and scattering from a fluid-elastic interface. The scheme is shown to be effective for these problems. The accuracy and stability is insensitive to the Poisson ratio. For the class of problems considered here we find that the fourth order scheme requires from two-thirds to one-half the resolution of a typical second order scheme to give comparable accuracy.

17. Key Words (Suggested by Authors(s))	18. Distribution Statement
elastic wave equation, fourth order accurate seismology,	64 - Numerical Analysis Unclassified - unlimited

19. Security Classif.(of this report)	20. Security Classif.(of this page)	21. No. of Pages	22. Price
Unclassified	Unclassified	44	A03

For sale by the National Technical Information Service, Springfield, Virginia 22161

NASA-Langley, 1986